Supporting Information For:

# Self-assembly of non-macrocyclic triangular $Ni_3Ln$ clusters

Tyson N. Dais,† Rina Takano,‡ Takayuki Ishida,‡ and Paul G. Plieger*†

† School of Fundamental Sciences, Massey University, Private Bag 11 222, Palmerston North, New Zealand.

‡ Department of Engineering Science, Graduate School of Informatics and Engineering, The University of Electro-Communications, 1-5-1 Chofugaoka, Chofu, Tokyo 182-8585, Japan.

* E-mail: p.g.plieger@massey.ac.nz

## Table of Contents

**Table S1.** Crystal structure and refinement details for complexes **C1** – **C4**. CCDC deposition numbers 2116396 – 2116399.

| **Complex** | **C1** | **C2** | **C3** | **C4** |
|---|---|---|---|---|
| **Deposition number** | 2116396 | 2116398 | 2116399 | 2116397 |
| **Molecular formula** | $C_{38}H_{46}LaN_3Ni_3O_{33}$ | $C_{37.5}H_{36}EuN_3Ni_3O_{28.5}$ | $C_{45}H_{54}GdN_3Ni_3O_{30}$ | $BaC_{43}H_{52}N_2Ni_3O_{28}$ |
| **Formula weight** | 1387.82 | 1312.78 | 1450.29 | 1358.33 |
| **Temperature /K** | 100 | 100 | 100 | 100 |
| **Crystal system** | monoclinic | monoclinic | monoclinic | triclinic |
| **Space group** | $P2_1/n$ | $C2/c$ | $P2_1/n$ | $P\bar{1}$ |
| **a /Å** | 10.4295(8) | 12.7986(12) | 17.0721(10) | 11.0862(6) |
| **b /Å** | 19.2819(15) | 16.5467(16) | 18.7861(11) | 15.5290(9) |
| **c /Å** | 24.0313(18) | 39.9720(4) | 17.1302(10) | 16.8872(9) |
| **α /°** | 90 | 90 | 90 | 115.311(4) |
| **β /°** | 102.277(3) | 90.203(3) | 106.716(3) | 101.491(4) |
| **γ /°** | 90 | 90 | 90 | 97.235(4) |
| **Volume /Å$^3$** | 4722.2(6) | 8464.9(14) | 5261.8(5) | 2501.3(3) |
| ***Z*/*Z'*** | 4 / 1 | 8 / 1 | 4 / 1 | 2 / 1 |
| **$\rho_{calc}$ /g cm$^{-3}$** | 1.952 | 2.06 | 1.831 | 1.804 |
| **μ /mm$^{-1}$** | 9.197 | 12.934 | 10.111 | 8.159 |
| **F(000)** | 2800 | 5256 | 2932 | 1376 |
| **Crystal size /mm** | 0.24 × 0.18 × 0.04 | 0.18 × 0.14 × 0.10 | 0.23 × 0.10 × 0.10 | 0.21 × 0.20 × 0.16 |
| **Radiation** | $CuK_\alpha$ ($\lambda$ = 1.54178) | $CuK_\alpha$ ($\lambda$ = 1.54178) | $CuK_\alpha$ ($\lambda$ = 1.54178) | $CuK_\alpha$ ($\lambda$ = 1.54178) |
| **2Θ range /°** | 5.93 to 136.49 | 4.42 to 136.46 | 6.44 to 136.48 | 6.03 to 136.48 |
| **Reflections collected** | 28526 | 129662 | 143215 | 68979 |
| **Independent reflections** | 8337 | 7697 | 9641 | 8850 |
| **Restraints/parameters** | 4 / 730 | 14 / 682 | 70 / 799 | 21 / 678 |
| **GooF on F$^2$** | 1.081 | 1.046 | 1.025 | 1.056 |
| **Final R indices [I ≥ 2σ(I)]** | $R_1$ = 0.0580, $wR_2$ = 0.1659 | $R_1$ = 0.0249, $wR_2$ = 0.0674 | $R_1$ = 0.0232, $wR_2$ = 0.0607 | $R_1$ = 0.0771, $wR_2$ = 0.1548 |
| **Final R indices [all data]** | $R_1$ = 0.0607, $wR_2$ = 0.1719 | $R_1$ = 0.0250, $wR_2$ = 0.0675 | $R_1$ = 0.0242, $wR_2$ = 0.0613 | $R_1$ = 0.1034, $wR_2$ = 0.1672 |
| **Residual density / e$^-$ Å$^{-3}$** | 1.92/-2.27 | 0.68/-0.72 | 0.76/-0.57 | 1.23/-1.28 |

**Table S2.** Selected distances and angles for **C1** – **C4**.

| Distance / Å | C1 | C2 | C3 | C4 | $Ni_3DyL'_3$ | $Ni_3YbL'_3$ |
|---|---|---|---|---|---|---|
| $Ln^{III} – O_{phenol}$ | 2.544(4) – 2.597(4) | 2.473(2) – 2.543(2) | 2.493(2) – 2.525(2) | 2.686(6) – 2.752(6) | 2.478(3) – 2.500(4) | 2.449(5) – 2.478(6) |
| $Ln^{III} – O_{nitrate}$ | 2.614(4) – 2.658(4) | 2.487(2) – 2.555(2) | 2.455(2) – 2.516(2) | 2.824(8) – 3.306(7) | 2.459(5) – 2.514(5) | 2.404(7) – 2.463(7) |
| $Ln^{III} – O_{water}$ | 2.515(4) | — | — | 2.881(9) | — | — |
| $Ni^{II} – O_{phenol}$ | 1.978(4) – 2.003(4) | 1.963(2) – 1.999(2) | 1.962(2) – 1.993(2) | 1.990(6) – 2.015(6) | 1.961(4) – 1.988(4) | 1.961(6) – 1.982(5) |
| $Ni^{II} – O_{formyl}$ | 1.983(4) – 2.016(4) | 1.981(2) – 2.008(2) | 1.975(2) – 2.023(2) | 1.990(6) – 2.013(6) | 2.004(4) – 2.017(4) | 2.000(7) – 2.011(6) |
| $Ni^{II} – O_{water}$ | 2.073(4) – 2.169(4) | 2.076(2) – 2.167(2) | — | 2.067(6) – 2.112(6) | — | 1.983(16) – 2.080(30) |
| $Ni^{II} – O_{methanol}$ | 2.098(4) | — | 2.061(2) – 2.120(2) | 2.068(7) – 2.099(7) | 2.050(5) – 2.098(6) | 2.055(7) – 2.237(15) |
| Av. $Ni^{II} \cdots Ni^{II}$ | 6.339(2) | 6.276(1) | 6.296(1) | 6.404(3) | 6.364(3) | 6.342(3) |
| Av. $Ni^{II} \cdots Ln^{III}$ | 3.670(2) | 3.625(1) | 3.636(1) | 3.761(2) | 3.675(3) | 3.662(3) |
| Min. $Ln^{III} \cdots Ln^{III}$ | 9.160(1) | 9.767(1) | 10.216(1) | 10.430(1) | 9.912(2) | 9.900(2) |
| **Angle / °** | | | | | | |
| $Ni^{II} – O – Ln^{III}$ | 105.6(2) – 107.3(2) | 106.2(1) – 108.7(1) | 106.1(1) – 108.9(1) | 102.6(2) – 105.4(2) | 109.8(2) – 110.9(2) | 110.2(2) – 111.2(2) |

**Table S3.** List of π—π interactions with centroid-centroid distances and angles, as calculated by Olex2. The second plane in each row corresponds to a symmetry generated molecule.

| Complex | Planes | $d_{centroid-centroid}$ /Å | Angle /° |
|---|---|---|---|
| C1 | ⟨C1, C2, C3, C4, C5, C6⟩<br>⟨C25, C26, C27, C28, C29, C30⟩ | 3.519 | 5.130 |
| | ⟨C41, C42, C43, C44, C45, C50⟩<br>⟨C25, C26, C27, C28, C29, C30⟩ | 3.597 | 4.422 |
| C2 | ⟨C41, C42, C43, C44, C45, C50⟩<br>⟨C45, C46, C47, C48, C49, C50⟩ | 3.668 | 8.272 |
| | ⟨C21, C22, C23, C24, C25, C30⟩<br>⟨C25, C26, C27, C28, C29, C30⟩ | 3.820 | 3.426 |
| | ⟨C1, C2, C3, C4, C5, C10⟩<br>⟨C25, C26, C27, C28, C29, C30⟩ | 3.885 | 18.729 |
| | ⟨C41, C42, C43, C44, C45, C50⟩<br>⟨C41, C42, C43, C44, C45, C50⟩ | 3.960 | 8.900 |
| C3 | ⟨C1, C2, C3, C4, C5, C10⟩<br>⟨C5, C6, C7, C8, C9, C10⟩ | 3.606 | 5.855 |
| | ⟨C5, C6, C7, C8, C9, C10⟩<br>⟨C5, C6, C7, C8, C9, C10⟩ | 3.723 | 0.000 |
| C4 | ⟨C1, C2, C3, C4, C5, C10⟩<br>⟨C25, C26, C27, C28, C29, C30⟩ | 3.580 | 3.674 |
| | ⟨C21, C22, C23, C24, C25, C30⟩<br>⟨C25, C26, C27, C28, C29, C30⟩ | 3.714 | 4.300 |

**Table S4.** Calculated high-temperature-limit values per ion and per molecule for **C1** – **C3**.

Per ion

| M | $J$ ($S$) | $g_J$ (calc.) | $\chi_m T$ / cm$^3$ K mol$^{-1}$ (calc.) | $M_{sat}$ / $\mu_B$ (calc.) |
|---|---|---|---|---|
| $Ni^{II}$ | 1 | 2 | 1.000 | 2 |
| $Eu^{III}$ | 0 | - | 0 | 0 |
| $Gd^{III}$ | 7/2 | 2 | 7.875 | 7 |

Per molecule

| Complex | $\chi_m T$ / cm$^3$ K mol$^{-1}$ (calc.) | $\chi_m T$ (calc.) | $M_{sat}$ / $\mu_B$ (exp. at 7 T) | $M_{sat}$ / $\mu_B$ (calc.) |
|---|---|---|---|---|
| **C2** | 7.57 (5000 Oe)<br>7.49 (500 Oe)<br>7.49 (500 Oe, in eicosane) | 3.00 | 8.07 (1.8 K, in eicosane) | 6 |
| **C3** | 12.68 (5000 Oe)<br>12.45 (500 Oe)<br>12.40 (500 Oe, in eicosane) | 10.88 | 13.66 (1.8 K, in eicosane) | 14 |

**Fitting parameters, $A$ and $B$, for the van Vleck equation used to fit $\chi_m T$ vs $T$ plot for C3**

$$A = 3exp\left(-48J/k_B\right) + 30exp\left(-45J/k_B\right) + 105exp\left(-40J/k_B\right) + 60( + 315exp\left(-30J/k_B\right) + 504exp\left(-27J/k_B\right) + 495exp\left(-24J/k_B\right) + + 990exp\left(-18J/k_B\right) + 1485exp\left(-14J/k_B\right) + 858exp\left(-13J/k_B\right) \quad \textbf{(1)}$$

$$B = exp\left(-48J/k_B\right) + 2exp\left(-45J/k_B\right) + 3exp\left(-40J/k_B\right) + 4exp\left(-3 + 8exp\left(-27J/k_B\right) + 5exp\left(-24J/k_B\right) + 12exp\left(-23J/k_B\right) + 4exp( \left(-14J/k_B\right) + 6exp\left(-13J/k_B\right) + 12exp\left(-7J/k_B\right) + 7 \quad \textbf{(2)}$$

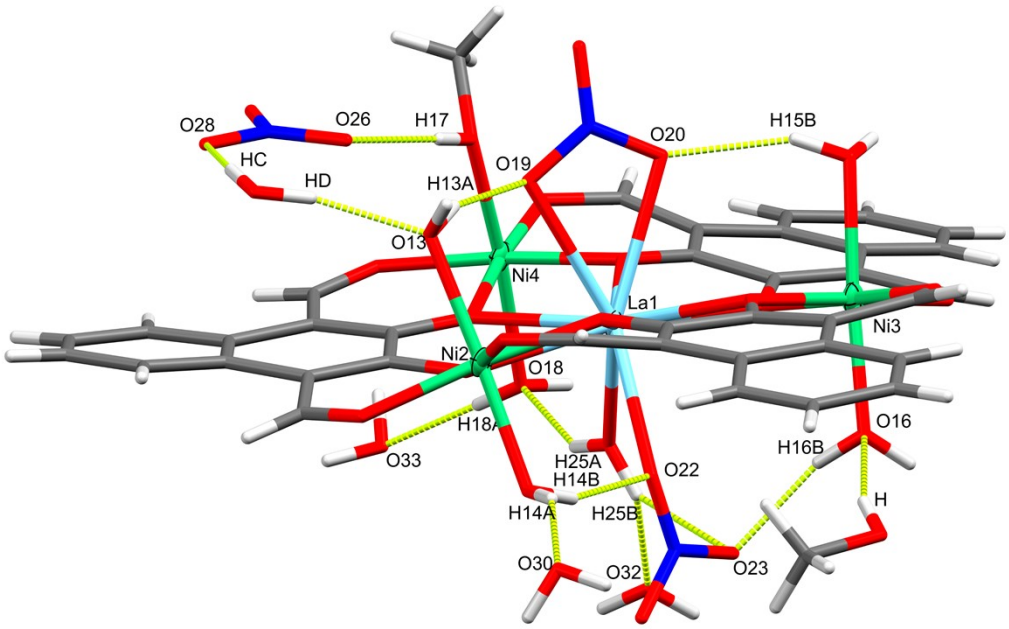


**Figure S1.** X-ray crystal structure showing the full asymmetry unit of **C1**. Thermal ellipsoids of metal atoms shown at the 70% probability level. C = grey, O = red, N = blue, H-bonds = yellow.

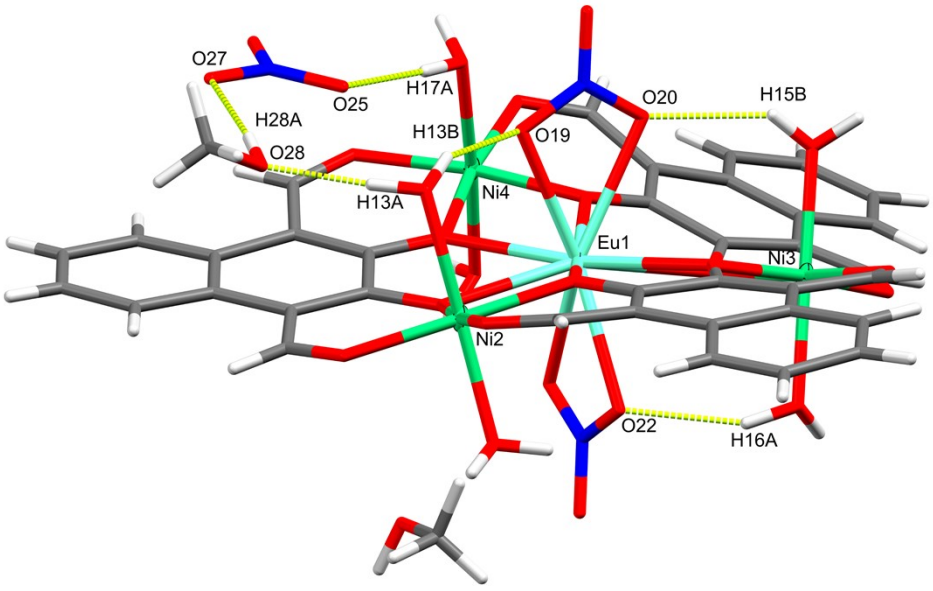


**Figure S2.** X-ray crystal structure showing the full asymmetry unit of **C2**. Thermal ellipsoids of metal atoms shown at the 70% probability level. C = grey, O = red, N = blue, H-bonds = yellow.

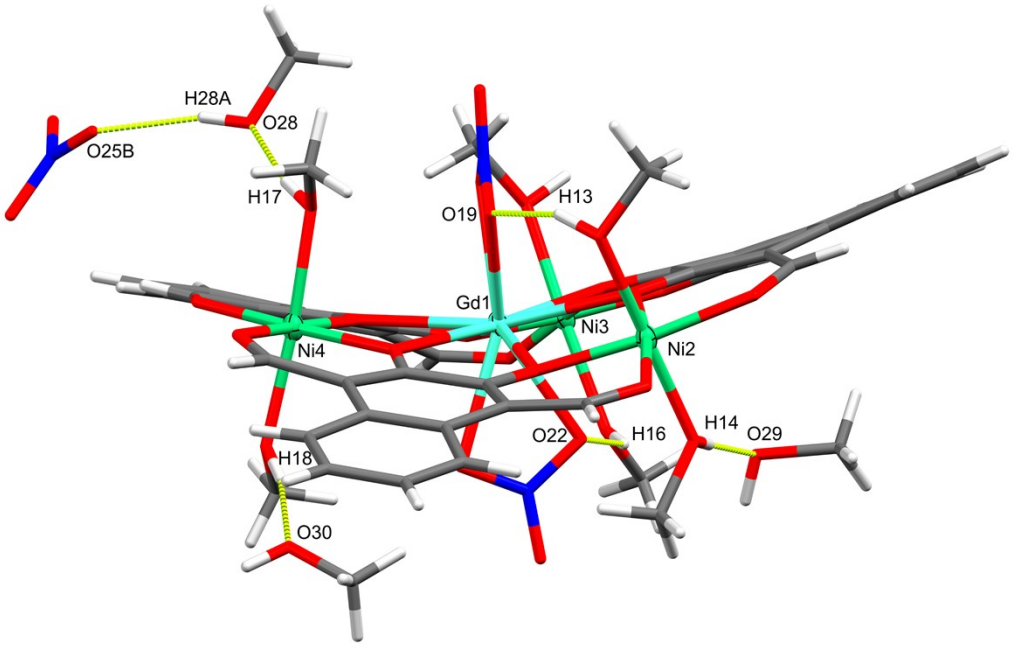


**Figure S3.** X-ray crystal structure showing the full asymmetry unit of **C3**. Thermal ellipsoids of metal atoms shown at the 70% probability level. C = grey, O = red, N = blue, H-bonds = yellow.

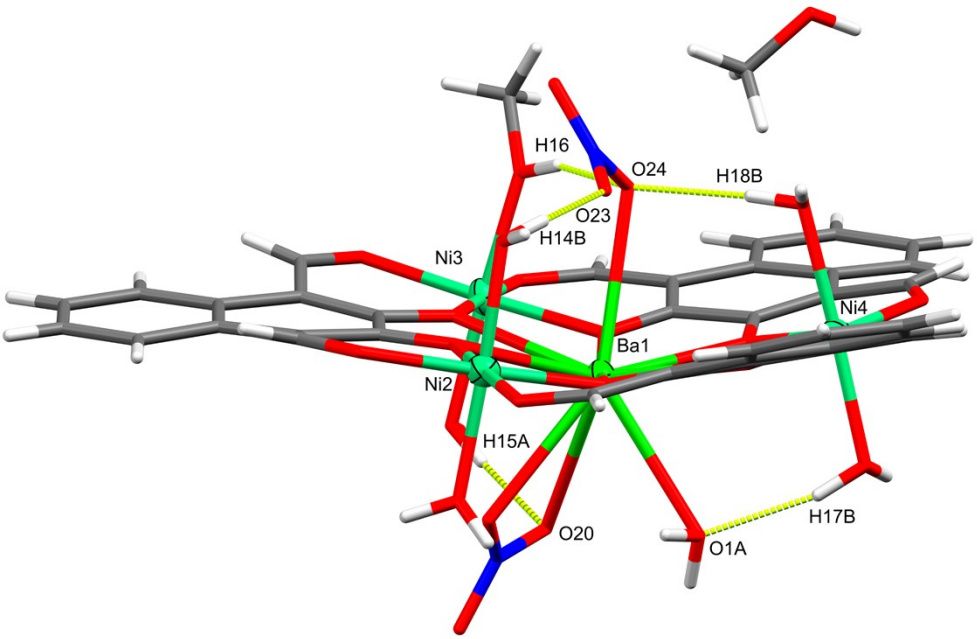


**Figure S4.** X-ray crystal structure showing the full asymmetry unit of **C4**. Thermal ellipsoids of metal atoms shown at the 70% probability level. C = grey, O = red, N = blue, H-bonds = yellow.

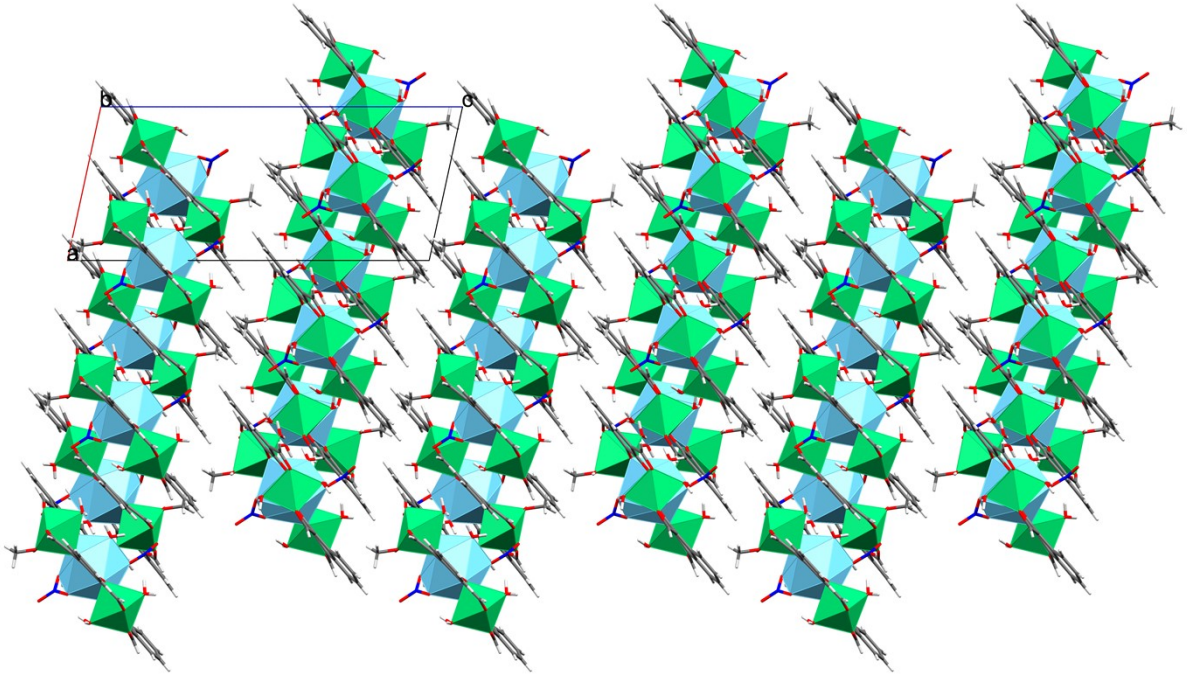

**Figure S5.** X-ray crystal packing diagram (3x3x3) of **C1**.

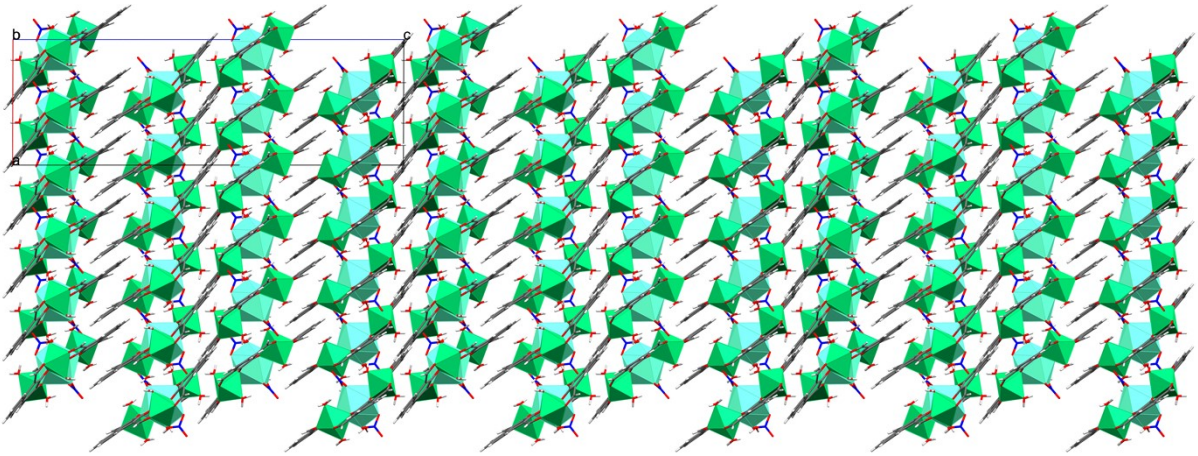

**Figure S6.** X-ray crystal packing diagram (3x3x3) of **C2**.

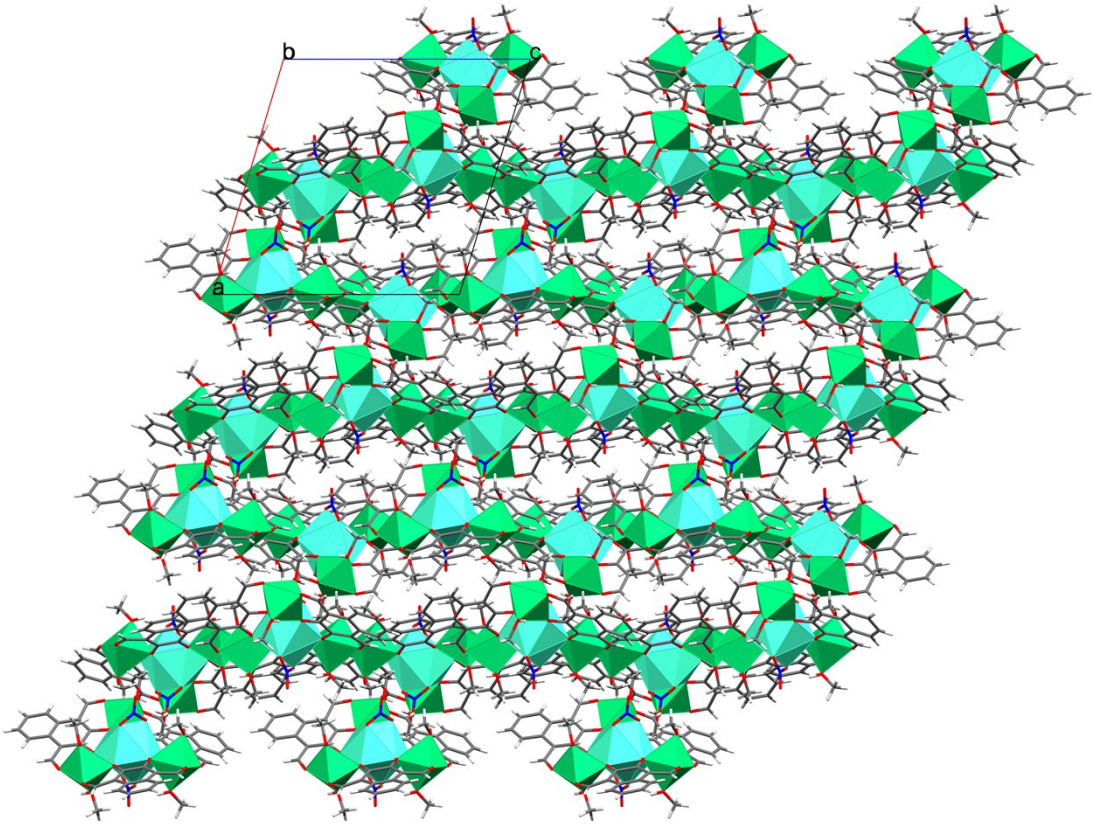


**Figure S7.** X-ray crystal packing diagram (3x3x3) of **C3**.

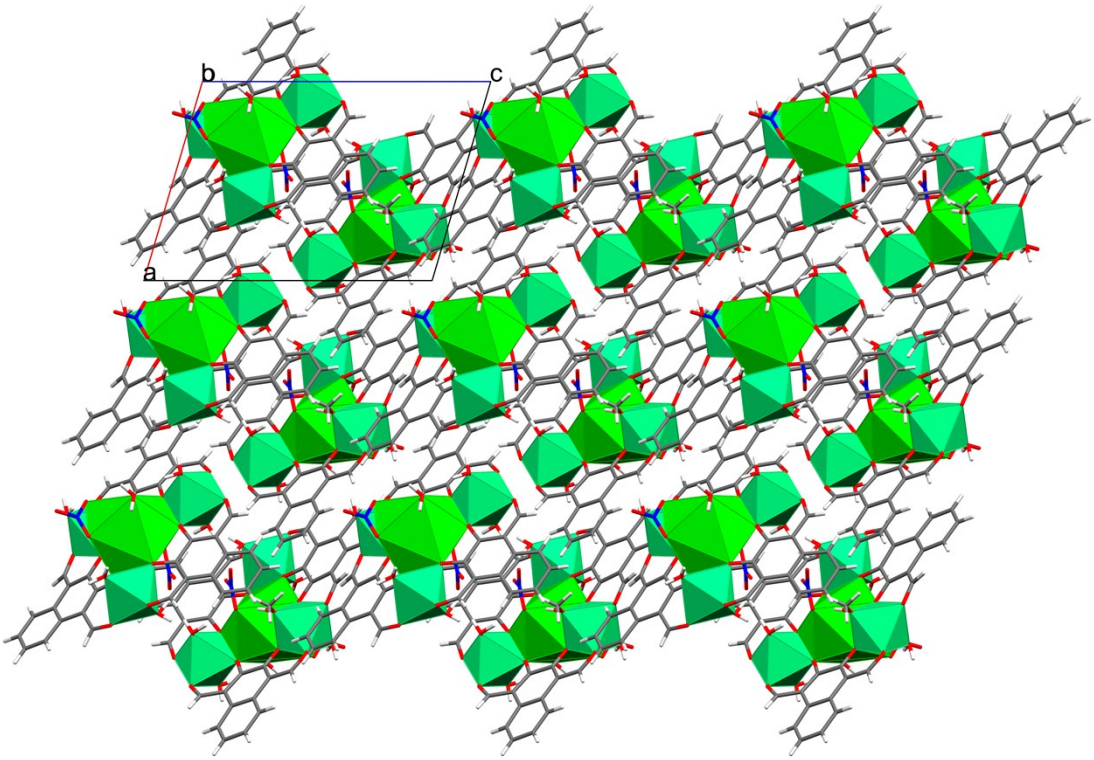


**Figure S8.** X-ray crystal packing diagram (3x3x3) of **C4**.

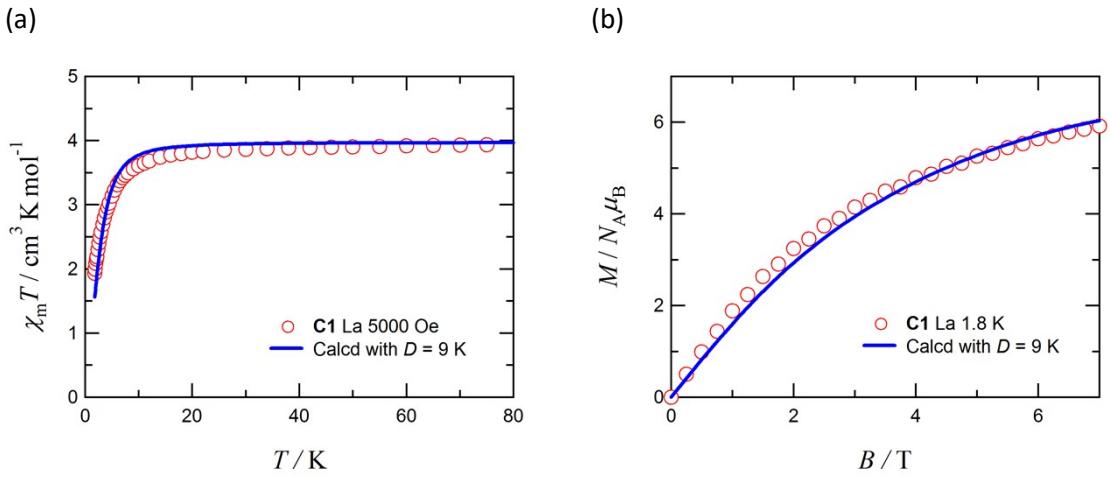


**Figure S9.** Simulation of the $\chi_m T(T)$ and $M(H)$ data on **C1** for optimization of $D$ with $g_{Ni}$ = 2.30.

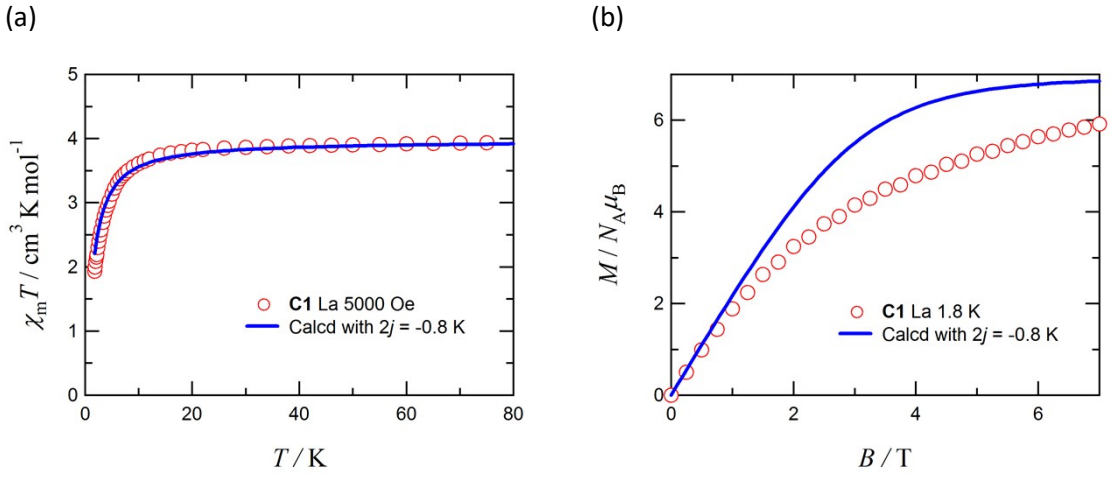


**Figure S10.** Simulation of the $\chi_m T(T)$ and $M(H)$ data on **C1** for optimization of $j_{Ni–Ni}$ with $g_{Ni}$ = 2.30.

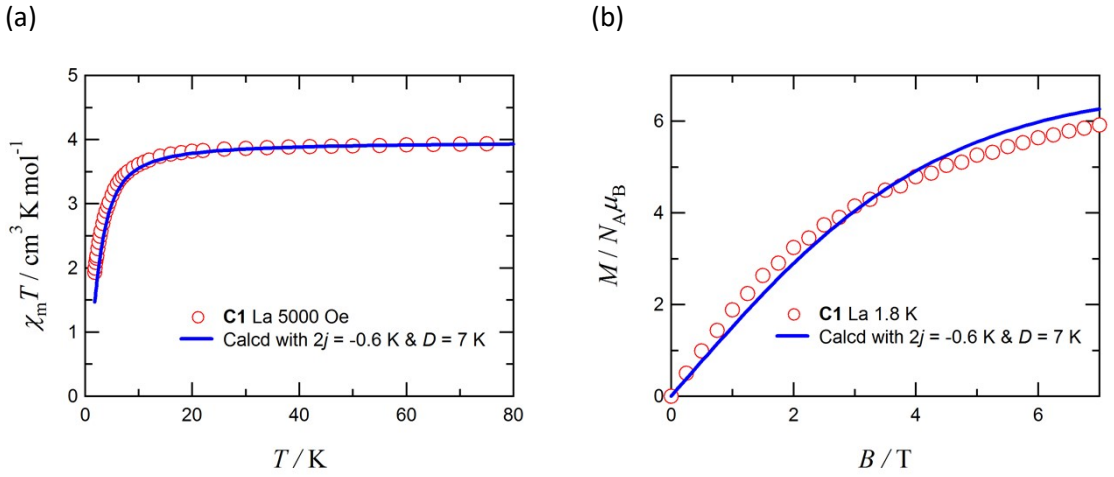


**Figure S11.** Simulation of the $\chi_m T(T)$ and $M(H)$ data on **C1** with $2j_{Ni–Ni}$ = –0.6 K, $D$ = 7 K, and $g_{Ni}$ = 2.30.

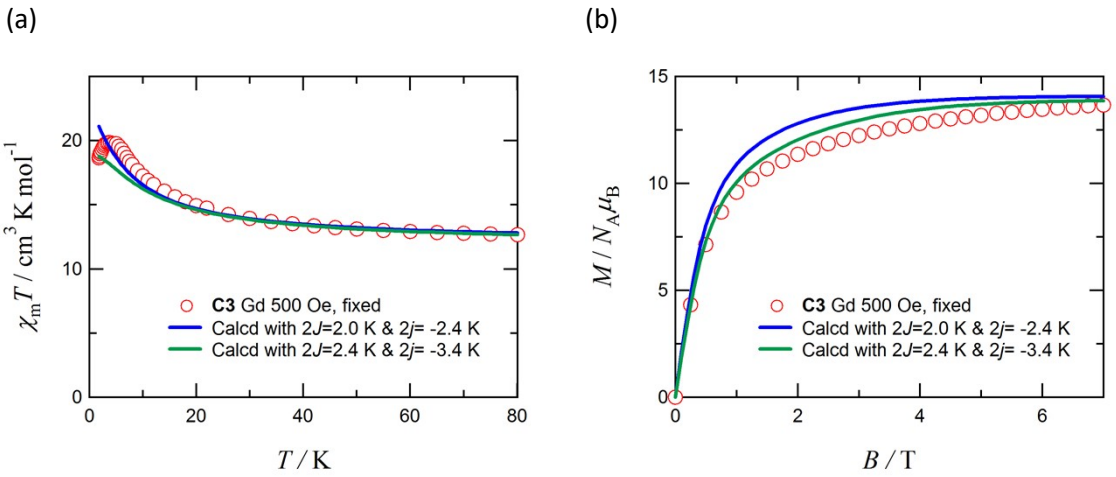


**Figure S12.** Simulation of the $\chi_m T(T)$ and $M(H)$ data on **C3** for optimization of $J$ and $j_{Ni–Ni}$ with $g_{Gd}$ = 2.00 and $g_{Ni}$ = 2.36 – 2.30.

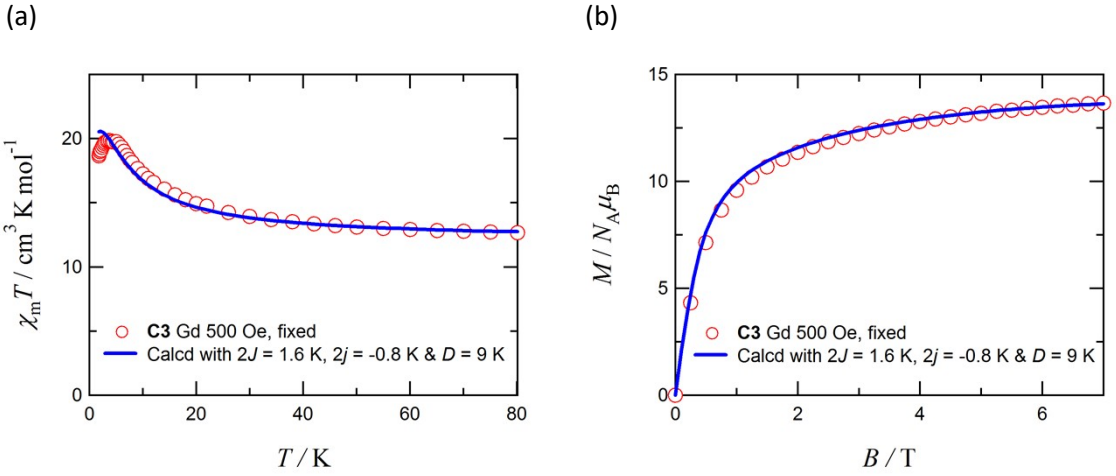


**Figure S13.** Simulation of the $\chi_m T(T)$ and $M(H)$ data on **C3** with $2J$ = 1.6 K, $2j_{Ni–Ni}$ = –0.8 K, $D$ = 9 K, $g_{Gd}$ = 2.00, and $g_{Ni}$ = 2.36.

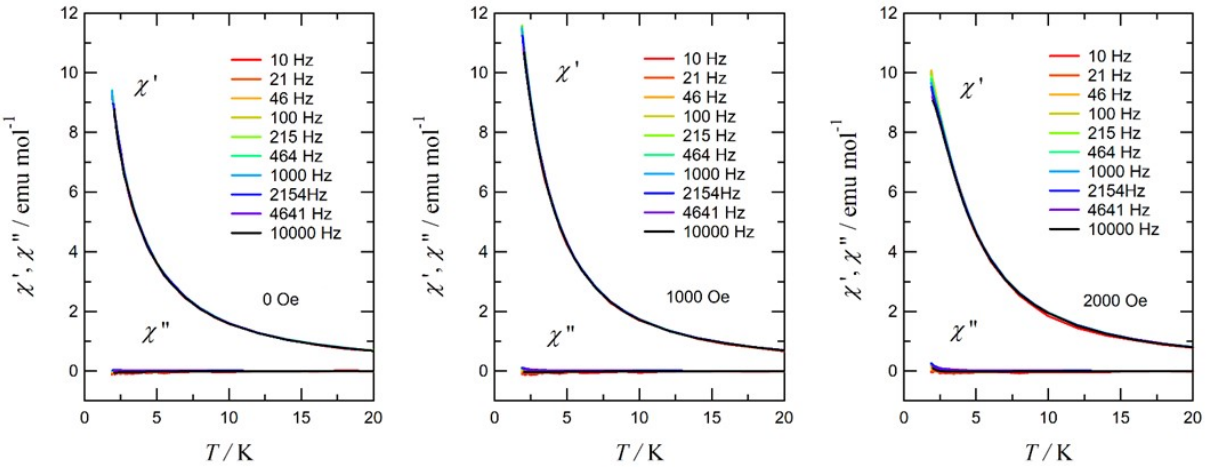


**Figure S14.** AC magnetic susceptibilities (in-phase χ' and out-of-phase χ") measured for **C3**. The applied dc bias fields (0, 1000, and 2000 Oe) are indicated. Lines are shown as a guide to the eye.